12-1-2023

Development of New High-Rate Shear Test Technique for Fiber-Reinforced Composites

Andrew Paul Baumgardner

Development of New High-Rate Shear Test Technique for Fiber-Reinforced Composites

by

Andrew Paul Baumgardner

An Honors Capstone

submitted in partial fulfillment of the requirements

for the Honors Diploma

to

The Honors College

of

The University of Alabama in Huntsville

1 December 2023

Honors Capstone Project Director: Dr. Nathan Spulak

11.29.2023

Student Date

Nathan Spulak Digitally signed by Nathan Spulak Date: 2023.11.29 13:40:35 -06'00' 11/29/2023

Project Director Date

George Nelson Digitally signed by George Nelson Date: 2023.11.30 09:09:57 -06'00' 11/30/2023

Department Chair Date

Digitally signed by Sean M Lane Date: 2023.11.30 16:00:36 -06'00'

Honors College Dean Date

Honors College

Frank Franz Hall

+1 (256) 824-6450 (voice)

+1 (256) 824-7339 (fax)

honors@uah.edu

Honors Thesis Copyright Permission

This form must be signed by the student and submitted with the final manuscript.

In presenting this thesis in partial fulfillment of the requirements for Honors Diploma or Certificate from The University of Alabama in Huntsville, I agree that the Library of this University shall make it freely available for inspection. I further agree that permission for extensive copying for scholarly purposes may be granted by my advisor or, in his/her absence, by the Chair of the Department, Director of the Program, or the Dean of the Honors College. It is also understood that due recognition shall be given to me and to The University of Alabama in Huntsville in any scholarly use which may be made of any material in this thesis.

___Andrew Baumgardner__________

Student Name (printed)

____

Student Signature

_____11.29.2023_________________

Date

Abstract

The shear strength of anisotropic materials under high-rate loading is a difficult property to measure. The goal of this project was to use finite element analysis and experimental testing to design a new high-rate shear test method for fiber-reinforced composites (FRCs). A better understanding of deformation of FRCs at high rate can improve the crashworthiness and resilience of aerospace structures and automobiles. This project involved iterating designs of a fixture to be used in a tension scenario in a load frame and in a split-Hopkinson bar to subject an FRC specimen to as pure shear as possible. This process involved simulation to verify the concept followed by machining iteration and testing. Digital Image Correlation systems were used to analyze the deformation and corroborated by physical measurements from the test hardware. The test was shown to be promising, but further testing of the design is necessary to judge its validity. Future use of this fixture and test approach can be used to improve simulation models of fiber-reinforced composites.

I. Introduction

Motivation/Scope. Fiber-reinforced composites (FRCs) are often used for their superior strength-to-weight ratio, and as such are often used in situations where extreme loading conditions apply. Armor, explosive ordinance containment devices, aerospace vehicles and high-end automotive components are all applications for these materials. The design of such devices requires in-depth knowledge of the deformation and fracture of FRCs at various strain rates. There exist many experimental methods for measuring shear, but they are unable to consistently induce shear fracture in FRCs at high strain rate due to their high anisotropy.

Background Research. One FRC shear test method is ASTM D5379 [1], known as the Iosipescu Shear Test. This test uses a rectangular flat strip specimen with symmetric v-notch in the center, as shown in Figure 1. The specimen is loaded in a custom fixture as shown in Figure 2.

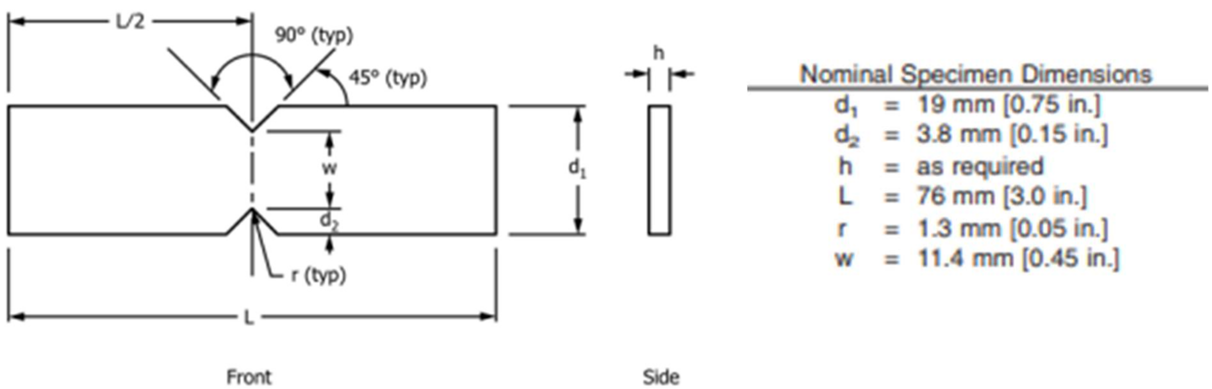

Figure 1. *Iosipescu Test Specimen* [1]

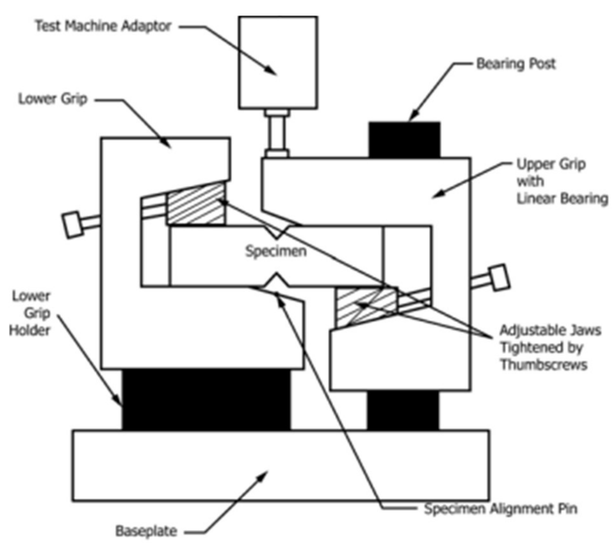

Figure 2. *Iosipescu Test Fixture Schematic* [1]

The Iosipescu test is sensitive to imperfections. Alignment issues in fixing the specimen can cause unwanted torsion, especially if the specimen thickness is too low. Its design is also founded on the assumption of homogeneous material, so it does not perform well on materials with rough features, such as a large fiber diameter or interwoven layers. Anisotropy also causes error when testing the *1-2* plane, which can be addressed using specialized shear strain gauges on the specimen or Digital Image Correlation as described in Section III. The Iosipescu test has common unacceptable and acceptable failure modes as shown in Figure 3.

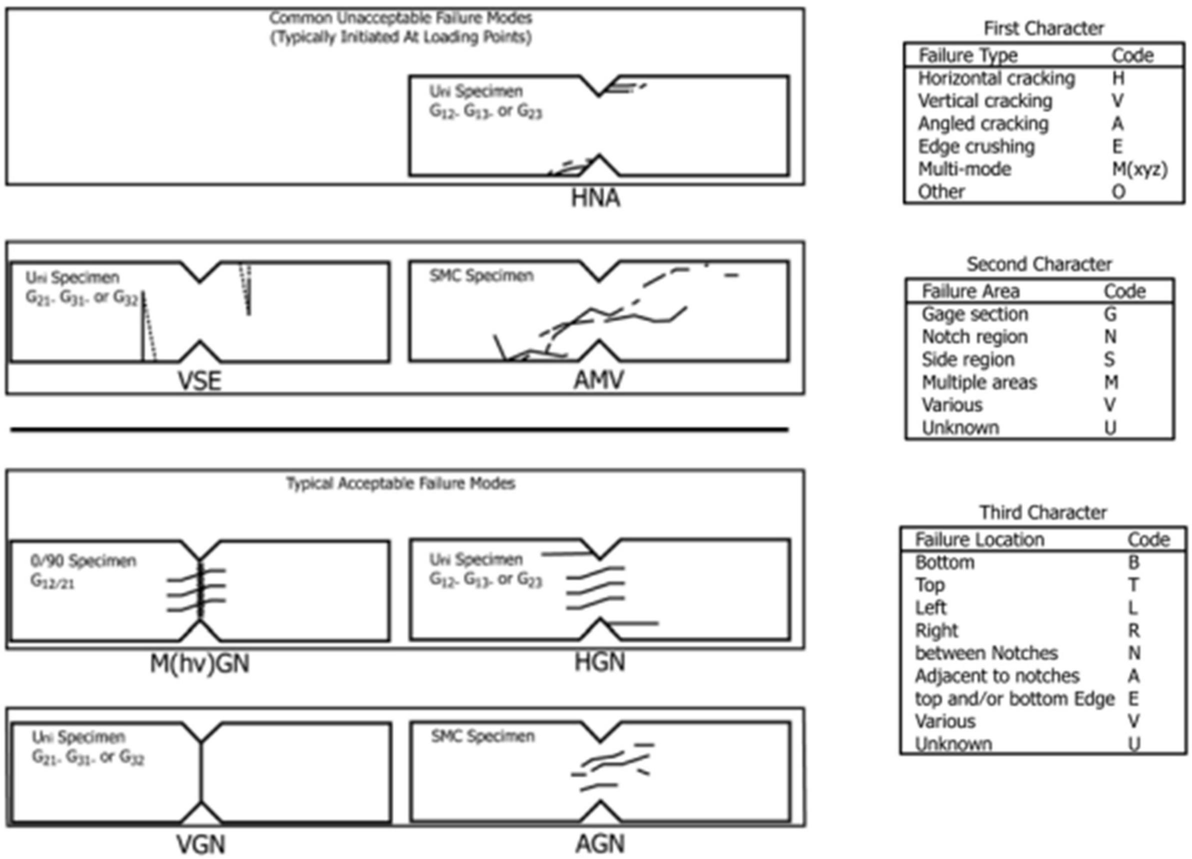

Figure 3. *Iosipescu Test Failure Modes/Codes* [1]

The primary reason the Iosipescu test is not sufficient for the desired test scheme is that the apparatus is not appropriate for high-rate testing. As described in Section III, the fixture for high-rate testing should be low in mass, complexity, and surfaces perpendicular to the primary force vector.

Other attempts have been made to design a test with this purpose. Yang (2016) devised a test which utilized a rectangular specimen with cutouts which cause a localized shear region in the gage section, as shown in Figure 4.

The test was found to be useful in some cases, but, when conducting test in the *1-2* plane, the stress localizations created by the cutouts caused delamination in the regions shown in red in Figure 5. Yang addressed this by sandwiching the specimen between steel covers which would help the specimen maintain integrity outside the gage section. This seems to have worked as intended, but visibility for Digital Image Correlation was reduced, and the scope of Yang's design did not include high-rate testing.

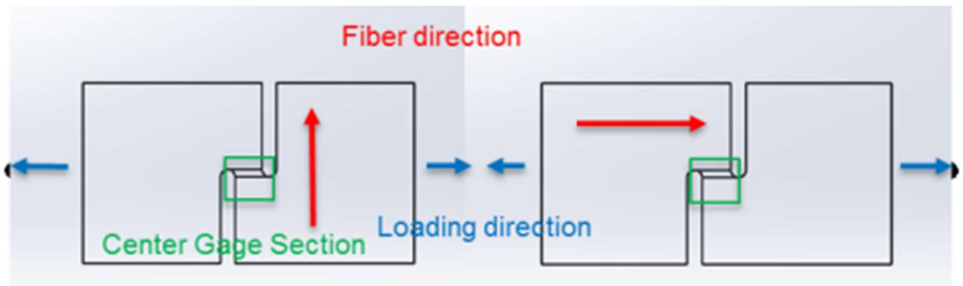

Figure 4. *Yang Test Design* [2]

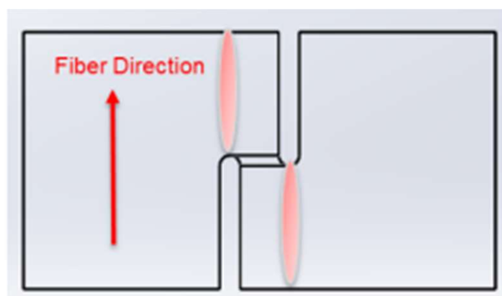

Figure 5. *Yang Test Failure Location* [2]

Experimenters Weng et al. (2020) devised a test which used a small cubic specimen in a hook-shaped grip. The test was ultimately very similar to that of Yang, but with the specimen being almost only the gage section. This reduced much of the challenge of machining the specimen without causing delamination or other such machining-related errors and reduced the amount of specimen material required to perform the test.

The first attempt involved a Z-shaped fixture as in Figure 6(a), but the gap was removed as in Figure 6(b) to improve alignment. Figure 6(c) shows the intended forces imposed on the specimen by the fixture during testing.

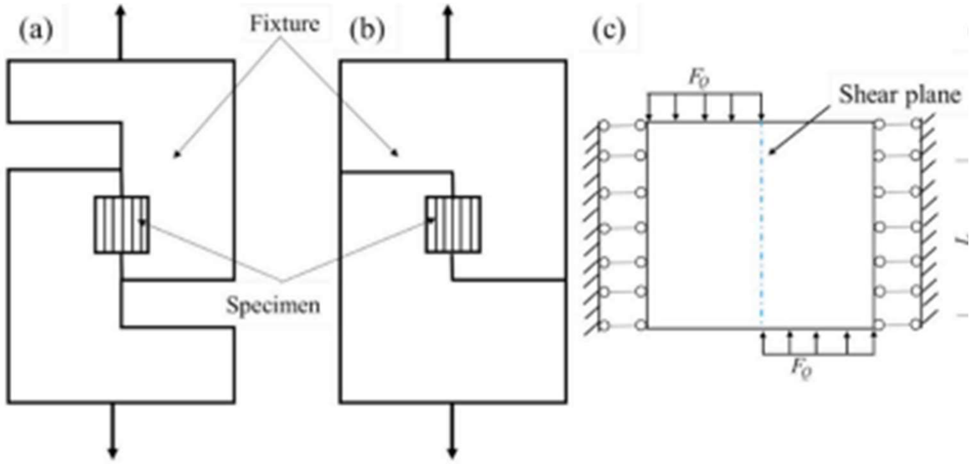

Figure 6. *Weng Shear Fixtures and Load Environment* [3]

Weng et al paired the load-displacement data from the load frame with Digital Image Correlation to determine that shear modulus increased with strain rate. The specimen loaded in the fixture in the load frame is depicted in Figure 7. The specimen is speckled as necessary for Digital Image Correlation.

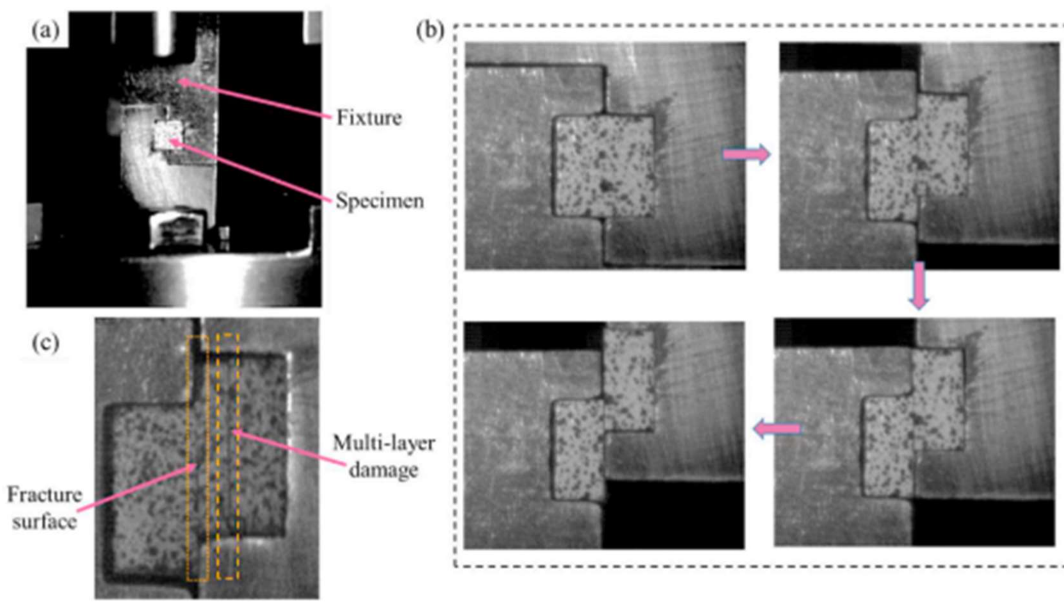

Figure 7. *Weng Shear Test (a) Platform (b) Specimen Failure Process (c) Damage at Strain Rate 1500s*$^{-1}$ [3]

Not shown in Figure 7 is the test platform for high-rate testing. The standard apparatus [4] for high-rate materials testing is the split-Hopkinson bar (SHB). This apparatus involves placing the specimen between cylindrical metal bars and striking the bars in a calibrated way to apply a measured impact wave to the specimen. The impact wave will reverberate through the bars, so the goal is to strike the specimen such that it fails after the first wave and record the entire deformation and fracture on a high-speed camera. Digital image correlation techniques can then be applied to the recording and compared to the data gathered from the wave to characterize the material's properties at different strain rates. The use of the split-Hopkinson bar and Digital Image Correlation is explained in greater detail in Section III.

II. Design and Simulation Analysis

Finite Element Analysis. It was necessary to validate designs in finite element analysis before dedicating physical resources to the test. LS-DYNA was used to simulate the test in the ideal case to justify the design of the test. The CAD model of the test fixture was imported into LS-DYNA as a STEP file and given the rigid material type. The bottom half of the fixture, which is red in Figure 9, was held in place in all 6 directions, while the top half, which is green in Figure 9, was prescribed a constant linear speed in the direction the test was meant to move and held rigid in the other 5 degrees of freedom. The test specimen was given the MAT_002 model (MAT_ORTHOTROPIC_ELASTIC), with which reasonable moduli of elasticity and shear moduli were used for each axis.

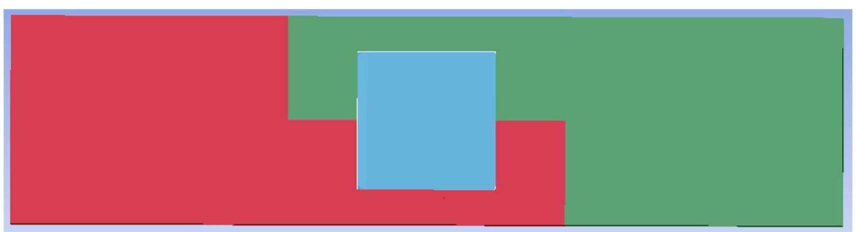

Figure 8. *Simulation Setup*

Many of the initial simulations showed that it was necessary to minimize the distance between the fixtures. When spacing was increased, shear effects began to become less focused and in-plane rotation became worse. Initially, the fixture was designed very simply, as in Figure 9(a), so that it was more easily machined. This design worked in the simulations because there was no out-of-plane perturbation.

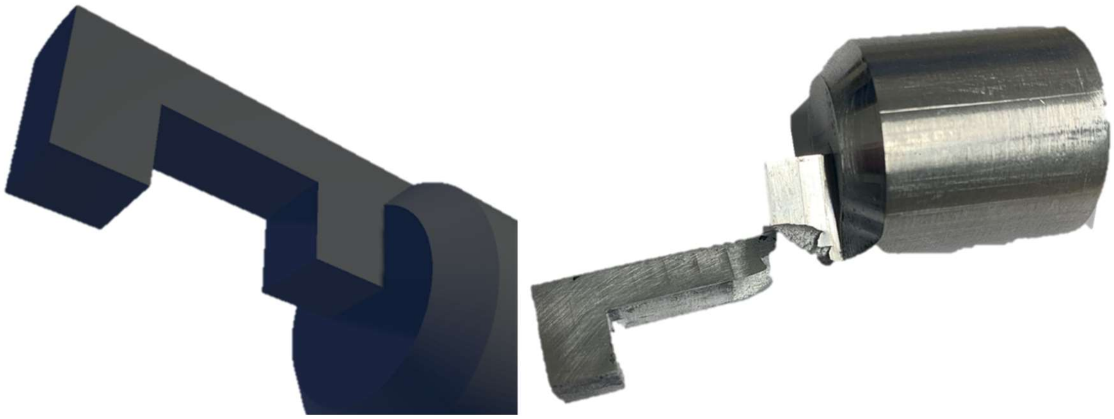

Figure 9. *Initial Design (a) and Failure (b)*

Early testing showed that the first design was flawed. When used in the split-Hopkinson bar, the specimen was ejected from the fixture due to out-of-plane effects. The two-part epoxy used to fix the specimen to the fixture was insufficient. Without the specimen in place, ringing caused by the load pulse and the ejection of the specimen caused the hook shapes of the fixtures to catch on each other and break one of them. It was determined that the next iteration of the design would need to restrict out-of-plane motion of the specimen, which would increase difficulty in machining. The "spine" of the shape would also be thicker to reduce ringing amplitude, as shown in Figure 10. Practical size restrictions of the split-Hopkinson bar called for the specimen size to be reduced to accomplish this.

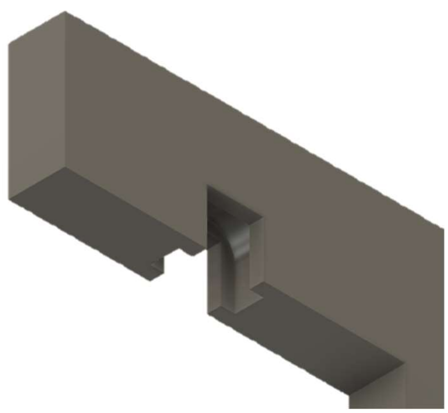

Figure 10. *Final Fixture Design*

The final design of the fixture included tabs around the specimen to keep it in place. The inside edges of the specimen slot needed to be rounded in order to be manufactured. This led to two specimen options: one which was also rounded to match the slot, or one that only reached the beginning of the fillet. New machining implements were required to machine the specimen without damaging the test material, so the second option was used for this project.

The tests were performed on specimens of commercially available polymer matrix fiber-reinforced composite and on specimens of solely polymer. The polymer was used as a proof of concept to investigate the differences in behavior between solely the matrix material and the matrix with addition of carbon fibers. This was useful in some stages of the process but did not reveal certain flaws that stem from the rigidity of the composite. Early tests with the polymer showed that out-of-plane movement would introduce error to the test, so JB-Weld brand two-part epoxy was used to fix the polymer to the fixtures. This change led to better results, but the epoxy strength was insufficient to control out-of-plane movement of the composite due to its superior strength: the stress the composite could endure under the same strain as the polymer far exceeded the strength of the epoxy. This led to the change in fixture geometry that can be seen between Figures 9 and 10. This fixture change was paired with a reduction in the specimen size. These changes allowed more bonding surface area for the epoxy and reduced the stress on the epoxy. The tolerance between the fixture slot and the specimen size was also very tight, allowing friction to share the load with the epoxy.

The addition of a gripping mechanism was considered. This mechanism would serve the purpose of the tabs added in Figure 10 but would be a separate piece that could be tightened down on the specimen. This option was not pursued primarily because it could not be applied to the split-Hopkinson bar. The added mass and flat surfaces would hinder the clean conduction of the load pulse.

III. Experimental Methods

Load Frame. An MTS 858 MiniBionix II load frame with hydraulic actuators and a two-axis calibrated load cell is used to apply forces to the test specimen. A common application of this tool is the dog-bone tension test, which uses a dog-bone shaped specimen which is fixed in the hydraulic grips of the load frame. The load frame lifts the top side while the bottom side does not move, which causes deformation primarily in the gage section of the specimen. Instead of fixing the specimen in the hydraulic grips, this experiment glues the specimen into the fixtures described in Section II and mounts the fixtures in the hydraulic grips. The fixtures are meant to redirect the tension forces from the into the specimen to create shear. The load frame is capable of applying and measuring torsion. The torsion axis will be locked during the experiment to ensure the only motion is axial so that shear is as isolated as possible.

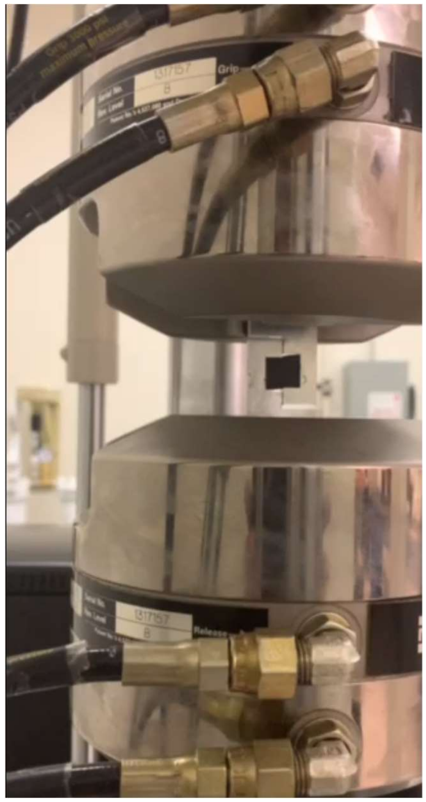

Figure 11. *Load Frame Test*

Split-Hopkinson Bar. The most common configuration of the split-Hopkinson bar is the compression configuration. With this setup, a specimen is lightly pressed between two cylindrical aluminum bars. On the opposite side of one of the bars is a pressure vessel, and on the opposite side of the other bar is a momentum blocker. The pressure vessel is loaded with a shorter bar, known as the striker bar, which is rapidly accelerated by the pressure vessel into the adjacent bar, known as the incident bar. This impact is transmitted through the incident bar as a load pulse at the speed of sound through that bar. Due to the wave dynamics, the load pulse is twice the length of the striker bar. The pulse is registered by a strain gage affixed to the incident bar which is calibrated to trigger a camera such that the camera can record the entire load pulse traveling through the specimen. Part of the load pulse is transmitted through the specimen and into the transmitter bar (which is then arrested by the momentum blocker), and the remainder of the wave is reflected back along the incident bar. The transmitted pulse is read by a second strain gage on the transmitter bar, and the reflected pulse is read again by the first strain gage. The readings from the two strain gages can be compared to determine how much energy was absorbed by the specimen and can be reconciled against Digital Image Correlation data from the high-speed camera recording to characterize the specimen deformation as a stress-strain curve. The bars and wave directions are shown in Figure 12.

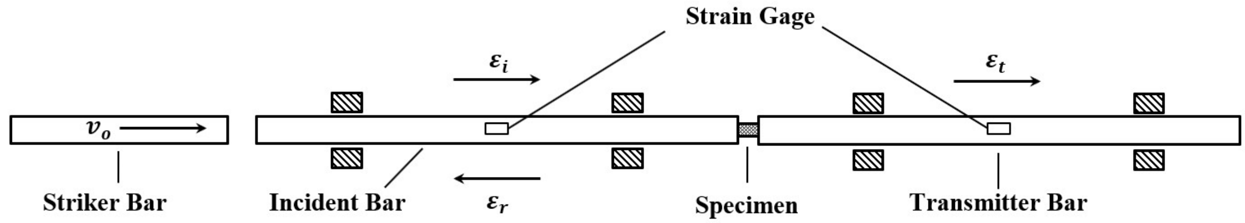

Figure 12. *Split-Hopkinson Bar Compression Configuration*

This test method uses a less common configuration of the SHB: tension. In this configuration, the pressure vessel is rotated 180° so that the striker bar is launched away from the specimen. The incident bar is given threads on either end and situated through the pressure vessel, and the striker bar becomes a tube around the incident bar. When it is fired away from the specimen, it strikes a collar on the incident bar to transmit a tension pulse to the specimen. The test configuration and wave directions are shown in Figure 13. The specimen is held in a tension grip, fixed to both bars with threading, as shown in Figure 14. The high-rate fixture designed for this test is designed to screw onto both bars and hold the specimen in place in view of the camera.

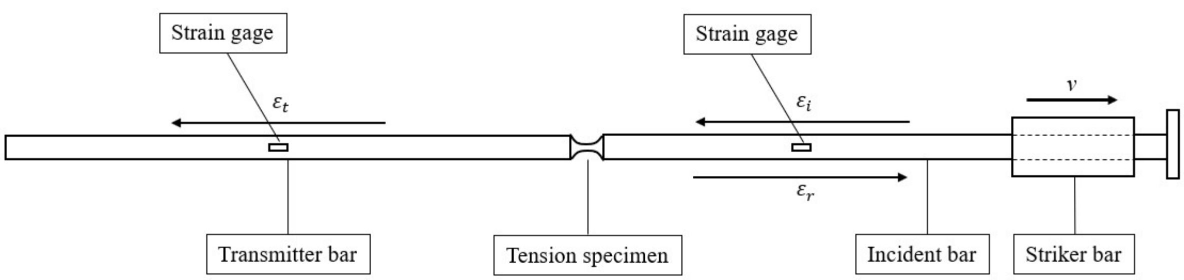

Figure 13. *Split-Hopkinson Bar Tension Configuration.*

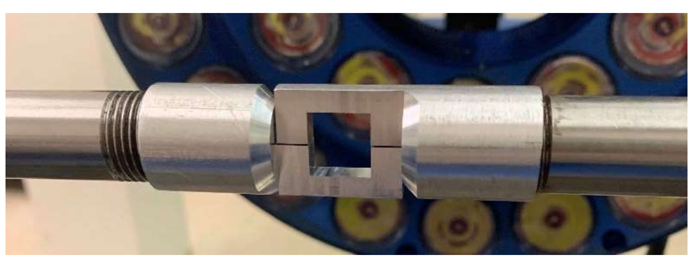

Figure 14. *Split-Hopkinson Bar Shear Fixture*

Digital Image Correlation. It is not practical to attach strain gages or extensometers to the specimen in this test. As such, a visual method must be employed to gather strain data on the specimen. Digital Image Correlation (DIC) involves painting the specimen with a near-random high-contrast pattern. Images taken during the test can be compared to the initial image to calculate strain. The software provided by Correlated Solutions represents the images with a brightness map based on a grid in the form of a spline field [5]. This allows the system to detect strains smaller than a pixel but is limited by the gradient. When painting the specimen, the goal is to make a high-contrast speckle pattern with the dots being roughly four pixels in diameter for the best results with this software. Figure 15 shows a tension test specimen with a near-ideal speckle pattern.

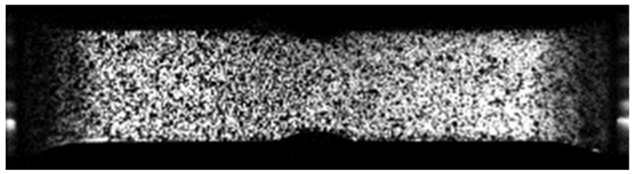

Figure 15. *DIC Tension Example*

For the high-rate tests with the split-Hopkinson bar, a high-speed camera was used. In order to capture an entire load pulse, light had to be maximized at the failure site, framerate increased, and the aperture opened. Due to the decreased focal range of a wider aperture, the specimen had to be at the right angle and the camera at the right distance to maximize focus and accuracy. The camera also had to be very carefully triggered so that it recorded the load pulse, since the high-speed camera used had a very limited recording capacity.

For the low-rate tests with the load frame, the camera setup was not as sensitive, so it was possible to use higher-resolution cameras. Two 2.3 Megapixel cameras were used in stereo, which allows the DIC software to generate a three-dimensional representation of the specimen. This allows data to be gathered of the out-of-plane motion, with much more detail than the in the high-rate test. This form of the test, however, requires much more careful calibration. Before each test, calibration panels are used in 30-50 images, as like those in Figure 16. The software has a record of the exact size of the panels, and generates an understanding of the spatial relationship between the two cameras. Throughout the test, both cameras take images simultaneously, as shown in Figure 17, and the software can use the model generated in calibration to represent the specimen in three dimensions.

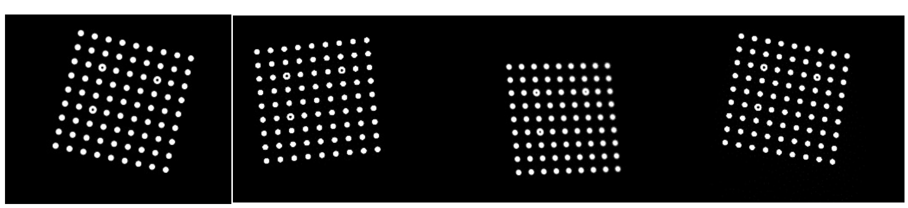

Figure 16. *Sample 3D DIC Calibration Images*

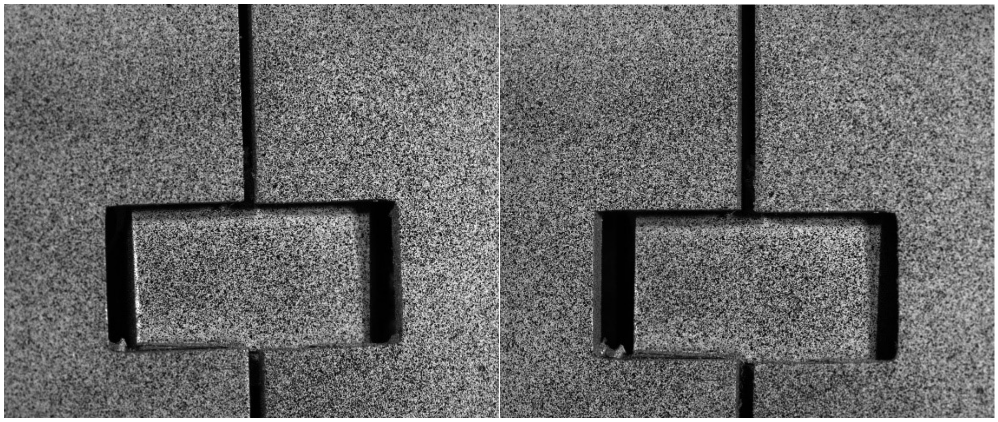

Figure 17. *Stereo Image Example*

The DIC software can graph any position-related data and superimpose it on the images taken. Properly paired with the load frame's load-displacement data, a stress strain curve can be generated.

Specimen Designs. The specimen was originally intended to be a half inch square of one eighth inch thickness, but the size was reduced to a quarter inch square of one eighth inch thickness after the first fixture fractured. The specimen was a commercially available unidirectional carbon-fiber-reinforced epoxy composite.

IV. Results

The low-rate experimental results demonstrate successful proof-of-concept for using the new test technique to induce fracture under shear loading in FRCs. Figure 18 shows that the data from the load frame corroborates the data from Digital Image Correlation. The shape of these curves is to be expected due to the failure characteristics of FRCs. The initial linear region is very steep and straight because the fibers are very strong, but when the fibers begin to fail, the whole specimen fails very suddenly, so there is not much data after the failure point.

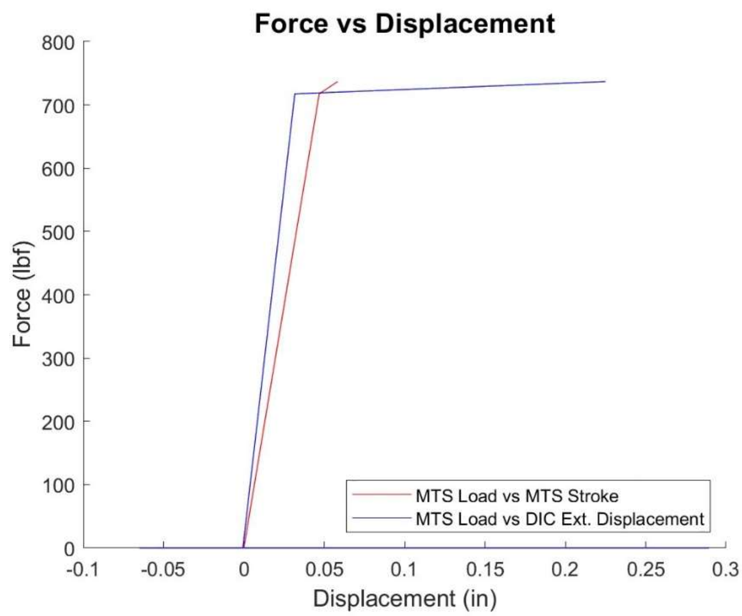

Figure 18. *Force-Displacement of Composite between Load Frame and DIC*

The below graph is the greatest indicator of the success of this test. Figure 19(a) is a color contour overlay of in-plane shear stress on top of the images gathered. The tightly grouped isolines show that the shear stress is highly localized in the intended region. Figure 19(c) is a horizontal cross section of the specimen. The high slope of the edges of the dip in the graph are a different representation of the tight isolines. These data express that the goal of creating localized shear in the gage region has been achieved. Furthermore, the shear stress in the gage region is relatively even in the gage section. Figure 19(b) is a vertical cross section of the specimen along the gage section. There are no major variations along the vertical axis, showing that shear is not strongly localized in an unwanted way.

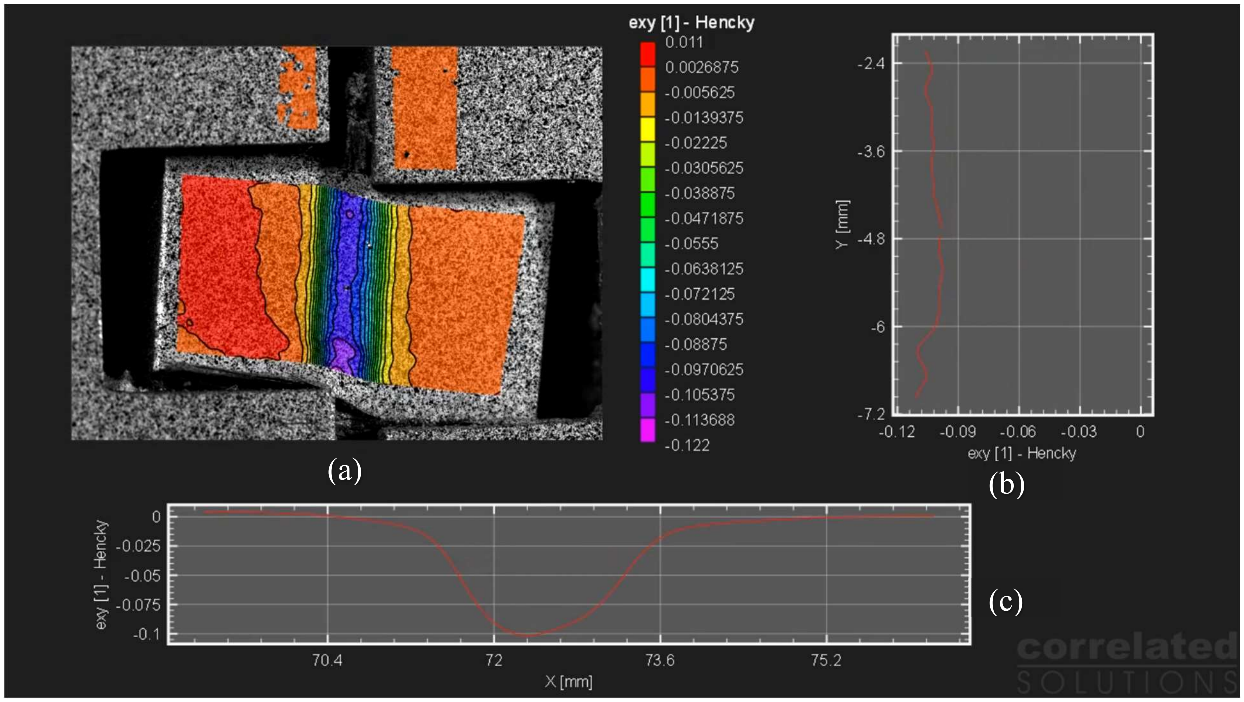

Figure 19. *DIC Data Visualized*

The practical test performed better than the LS-DYNA simulations predicted. The simulations were not capable of including the intricate interactions of the fibers on the small scale, only small representations of orthotropic cells. The fibers seem to have a stabilizing effect on stress throughout the specimen.

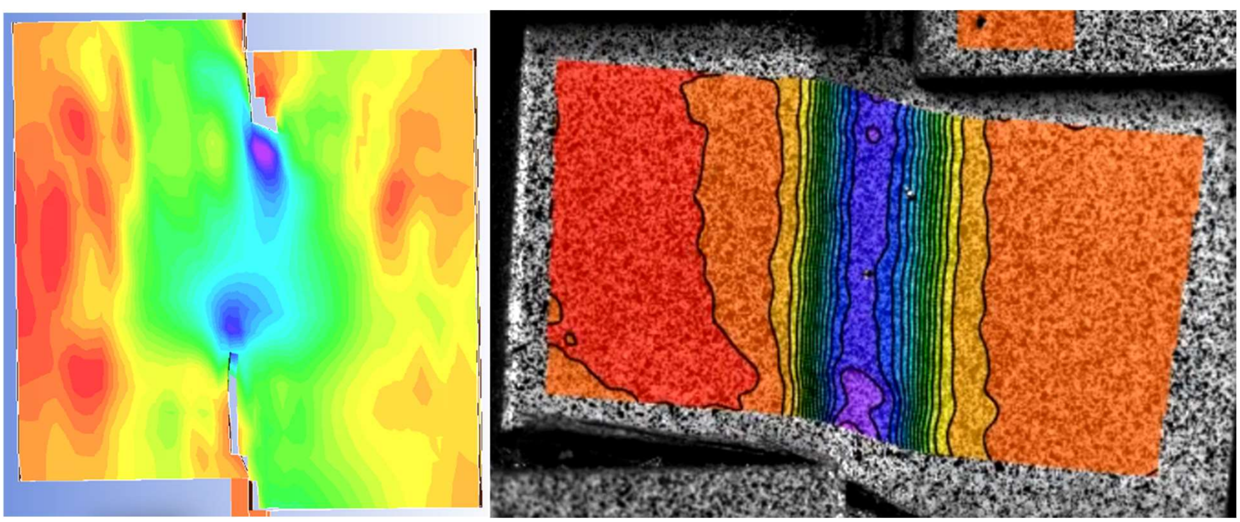

(a) ***(b)***

Figure 20. *Shear Strain Comparison Showing (a) Simulation and (b) DIC Test Data*

The dark spaces above and below the gage section are gaps between the fixtures. Decreasing the distance between the fixtures may improve shear localization, but this gap was created as a precaution so that ringing in the split-Hopkinson bar post-failure does not damage the test apparatus (See Figure 9(b)).

Future Use. Further experimentation is needed to validate this test design. Due to time constraints, this project was not able to perform high-rate tests using the second, finalized shear fixture design. Further repetition of testing with the load frame may expose yet unseen weaknesses in this test or improve the validity of the results. Literature so far disagrees as to the effects of strain rate on FRCs, with some claiming that increased strain rate increases shear strength [3], and others claiming a less determinate relationship [2]. Further experimentation with this less common test method may yield interesting, or more nuanced results. This test may also be modified to measure interlaminar shear stress, though it is not recommended to use the same stock material as used in this project. The fixtures would need to be modified or an FRC stock would need to be found with the fiber direction in line with the thickness axis.

V. Conclusion

In this project, a new fixture was designed with the intent of validating a less common form of shear test for anisotropic materials [3] which can be implemented in low- and high-strain rate experimentation. The test was simulated using finite element analysis and the design was iterated upon between the simulations and real-world testing. Low- and high-strain rate tests were performed with an initial design, and it was found that it is necessary to structurally support the specimen to prevent out-of-plane rotation. Digital Image Correlation techniques validated that the modified design successfully induced localized shear deformation and fracture on the FRC specimen. The test was found to perform better than expected, with shear strain more even and more localized than simulations predicted. The test is promising but requires further experimentation in low-rate scenarios and implementation in high-rate scenarios. As it is used in further testing, it may require further modification as necessary to similarly induce high strain rate shear deformation and fracture in FRCs. Future work with this test may provide better insight into the effects of strain rate on the shear strength of fiber-reinforced composites.

References

[1] ASTM International, "Standard Test Method for Shear Properties of Composite Materials by the V-Notched Beam Method," 2023.

[2] P. Yang, "Experimental Techniques and Mechanical Behavior of T800/F3900 at Various Strain Rates," The Ohio State University, 2016.

[3] Y. F. M. R. J. S. L. F. Fei Weng, "Effect of high strain rate on shear properties of fiber reinforced composites," vol. 203, 2020.

[4] H. Kolsky, "An investigation of the mechanical properties of materials at very high rates of loading," *Proceedings of the physical society,* vol. Section B, no. 62(11), p. 676, 1949.

[5] H. O. J. J. &. S. M. A. Schreier, Image correlation for shape, motion and deformation measurements: Basic concepts, theory and applications (Vol. 1), Boston, MA: Springer-Verlag US, 2009.